Localization and Path Planning for Railway Inspection Robot Based on Multi-Sensor Fusion and Improved ACO

YunFei WANG[1]*, MingLiang LIANG[1], YaRu ZHAO[2]

[1] Zhengzhou Railway Vocational and Technical College, Henan, 451460, China
wangyunfei3205@126.com (**Corresponding author*), lunwenzz@163.com

[2] Zhongyuan University of Technology, Henan, 451191, China
6641@zut.edu.cn

Abstract: In order to achieve the precise positioning of railway inspection robots and optimize their inspection paths, this paper focuses on robot work optimization for railway inspection environments. Firstly, an adaptive improvement strategy is proposed for the extended Kalman filter algorithm, and a multi-sensor information fusion-based positioning algorithm is implemented for railway inspection robots. Then, based on the improved ant colony optimization algorithm, a path planning model for inspection robots is constructed. The experimental results show that the multi-sensor information fusion-based positioning algorithm features a high positioning accuracy, and the positioning root mean square error converges to the minimum value of 0.136. To that, the inspection robot localization success rate and the stability of the proposed method make it better than other methods, with an increase in the success rate amounting to 29.41%. At the same time, the improved ant colony optimization-based path planning model achieves the highest planning efficiency, with a localization success rate of 97.35% in railway inspection environments with obstacles, a maximum reduction of the inspection path length amounting to 36.49%, an average planning time reduction of up to 46.67 seconds, and excellent path smoothness. The implementation of this positioning algorithm and path planning model helps improve the railway inspection efficiency and promotes the development of multi-sensor fusion technology.

Keywords: Inspection robot, Railway, Information fusion, Sensor, Ant colony optimization algorithm.

1. Introduction

The railway transportation lines in China exhibit the characteristics of being dense in the east and sparse in the west, widely distributed, connecting major urban agglomerations and core cities in China, and occupying a major position in the field of transportation in China. Regular railway inspections are of crucial importance in ensuring the safety of railway transportation and the smooth operation of trains (Moon et al., 2024; Stanojević & Stanojević, 2024). Through railway inspections, safety hazards in railway lines can be detected and eliminated in a timely manner, damaged parts on railway lines can be repaired, and operational delays or safety accidents caused by line problems can be avoided (Wang et al., 2023; Fan, 2024). However, traditional manual inspections involve high labor intensity, harsh working environments, and subjective judgment interference, which pose severe challenges to the railway inspection work (Xing, 2024). In recent years, railway line inspections have gradually relied on advanced technological means and instrument equipment. Robot inspections can overcome the shortcomings of manual inspections to a certain extent, and through high automation and intelligence, the risk of human errors can be effectively reduced. However, railway lines often traverse various complex terrains, obstacles, and harsh weather conditions that interfere with the sensor performance of inspection robots, significantly reducing their positioning accuracy. The existing research shows that multi-sensor fusion (MSF) technology can reduce the error of a single sensor by integrating data from different sensors, improve the environmental awareness of patrol robots, and thus improve the positioning accuracy. In addition, a good inspection path can help improve inspection efficiency and ensure a high inspection quality, but the existing path planning (PP) methods have a low adaptability to the characteristics of railway lines and inspection task requirements. At present, swarm intelligence optimization algorithms have been widely applied in different fields, especially the ant colony optimization (ACO) algorithm, which has shown a great potential in PP. However, it is still necessary to explore robot PP algorithms that are suitable for railway inspection. Therefore, to foster the intelligent advancement of the railway industry and provide a more accurate and efficient positioning and PP solutions for railway inspection robots, this paper first innovatively proposes an adaptive improvement strategy based on an extended Kalman filter (EKF), and describes how the construction of a MSF positioning algorithm is completed. Then, innovative improvements are made for the ACO, and the design of a robot PP algorithm is presented.

https://doi.org/10.24846/v34i4y202503

The remainder of this paper is structured as follows. Section 2 presents a review of the current research status on inspection robot positioning and PP at home and abroad. Section 3 elaborates on the construction process for the positioning algorithms and PP models, while Section 4 discusses the experimental results. Finally, Section 5 concludes this paper and outlines possible future research directions.

2. Related Works

Inspection robots have been widely used in various industries such as park inspection, the power industry, and petrochemicals, and have received extensive attention from researchers. Key technologies such as the positioning and PP of the inspection have been studied. In order to improve the coverage of the working area of power inspection robots, Jiang et al. (2023) focused on the challenges of intelligent control programs in navigation modeling and PP. By using multiple information fusion for simultaneous localization of railway inspection robots and map construction, Kalman filtering (KF), five-layer neural networks and fuzzy neural networks were employed, and high-precision localization and dynamic PP were achieved. The simulation verification showed that the algorithm was effective and accurate in complex environments, improving the efficiency of the inspection robot (Jiang et al., 2023). Li (2024) aimed at traffic congestion, accidents and environmental problems in the process of urbanization. An intelligent expressway traffic monitoring system based on the Internet of Things was proposed, and intelligent inspection robots were introduced to monitor road traffic flow and violation records in real time. The inspection robot utilizes deep learning and artificial intelligence technologies, combined with improved synchronous positioning and map construction algorithms. The results showed that the proposed method had a good computational efficiency (Li, 2024). Sugin Elankavi et al. (2023) designed two wheeled pipeline inspection robots in response to the limitations of traditional manual inspection methods and early robot designs, aiming to overcome the motion singularity problem at pipeline bends. They adopted wheels with asymmetrical angles to maintain contact with the pipe surface and avoid motion singularities. Through motion analysis and experimental verification, the proposed method showed a high stability and accuracy in pipeline inspection (Sugin Elankavi et al., 2023). Gilmour et al. (2023) designed a new robot track positioning method using a vehicle mounted depth camera for navigation in a semi-structured environment. The experimental results showed that this method had a high accuracy and was suitable for different materials and lighting conditions. Taking steel plate inspection as an example, it could accurately locate the track within a range of 5.7 mm, which was significantly better than traditional manual and existing robot solutions (Gilmour et al., 2023). To achieve an efficient inspection, Xie et al. (2024) proposed a relative positioning approach based on a radio frequency identification tag array. By deploying tag arrays in the detection area and constructing a fingerprint database, the high-precision positioning of inspection robots can be achieved. The experiments showed that this method was less affected by trajectories and obstacles, with a positioning error of less than 6 cm in complex scenes, effectively improving the inspection accuracy and efficiency (Xie et al., 2024).

Tang et al. (2024) proposed an improved artificial electric field algorithm for the problem of robot PP optimization. By introducing three mechanisms, namely parameter adaptation, reverse learning and Cauchy mutation, the exploration ability and convergence accuracy of the algorithm were improved. The article combines the improved artificial electric field algorithm with cubic spline interpolation to generate smooth and continuous paths, thereby solving the problem of global PP in a three-dimensional environment, and verifies the effectiveness of the algorithm through a large number of virtual simulation experiments (Tang et al., 2024). Xi et al. (2024) proposed a lightweight real-time PP method based on reinforcement learning for the optimization problem of unmanned aerial vehicle (UAV) PP - the adaptive soft actor-Critic algorithm. This method constructs a global training and local adaptation framework by optimizing the training process, network architecture and algorithm model, and introduces a cross-layer connection method to avoid feature loss and improve the learning efficiency. The results proved the superiority and adaptability of the proposed method in PP optimization (Xi et al., 2024). To tackle the communication challenge of mining industry robots in closed environments, Cid et al. (2024) proposed a semi-autonomous leader-follower scheme and a multi-robot connection perception system by using remote radio frequency to predict signal propagation and

PP. The experiments showed that this method significantly improved the communication quality and inspection range, achieving an effective operation in a line-of-sight environment (Cid et al., 2024). Lou et al. (2025) proposed a hybrid multi-strategy sandcat swarm optimization algorithm for the PP optimization problem of mobile robots. This algorithm improved the convergence accuracy through the nonlinear adjustment strategy, introduced the logarithmic weighting strategy to balance the exploration and exploitation capabilities of the algorithm in the search space, used the alternating selection strategy to jump out of the local extremum, and adopted the Levy flight position update formula to prevent the algorithm from getting stuck. The results showed that the proposed algorithm had a good planning effect (Lou et al., 2025). To optimize the PP of vehicles like mobile robots in complex scenes, Li et al. (2024) proposed a PP method based on an improved ACO algorithm and fractional-order models for non-smooth path problems in narrow and large-sized scenes, which improved the modeling accuracy and search efficiency, and achieved a smooth and efficient path generation (Li et al., 2024).

Overall, significant progress has been made with regard to the localization and PP of inspection robots, such as multi-information fusion positioning and intelligent algorithm-based optimization of paths, effectively improving the inspection efficiency and accuracy. However, for specific complex environments such as railway inspections, the existing technologies still face challenges, such as the ever-changing environment and dense obstacles along the railway. Therefore, research on the positioning and PP of railway inspection robots is particularly necessary, and adaptive exploration has been conducted using advanced technologies such as multi-information fusion positioning and intelligent algorithms.

3. Research Methodology

MSF technology and swarm intelligence algorithms can provide support for improving the key performance of inspection robots. The study first designed a robot positioning algorithm under the background of MSF, and then fused multiple swarm intelligence algorithms to construct a PP model.

3.1 The Proposed Positioning Algorithm

MSF technology can enhance the environmental perception ability and robustness of robots through redundant design. Research is been conducted on the design of robot positioning algorithms under MSF. The study first presents a kinematic model of the inspection robot, and the constructed coordinate system and corresponding positional relationship are shown in Figure 1.

As shown in Figure 1, the kinematic model of the robot includes two major coordinate systems: a local and a global system. The local coordinate system is centered around the robot and is used for helping the robot perceive and understand its surrounding environment. The global coordinate system belongs to a larger fixed reference framework that covers the overall range of motion of the robot, providing a unified and global perspective for the robot. The study uses the feature map method to define the motion environment of robots and represents the environment using the global position of parameterized features. Firstly, the study sets the known environmental feature point in the motion environment of the inspection robot, which is represented as $L_i = (x_i, y_i)$. A set of feature points form the environmental map feature set. The pose of a robot is composed of position coordinates and deflection angles in a two-dimensional plane, and its own pose can be estimated using the feature point $L_i = (x_i, y_i)$ (Jovanović et al., 2023; Pang et

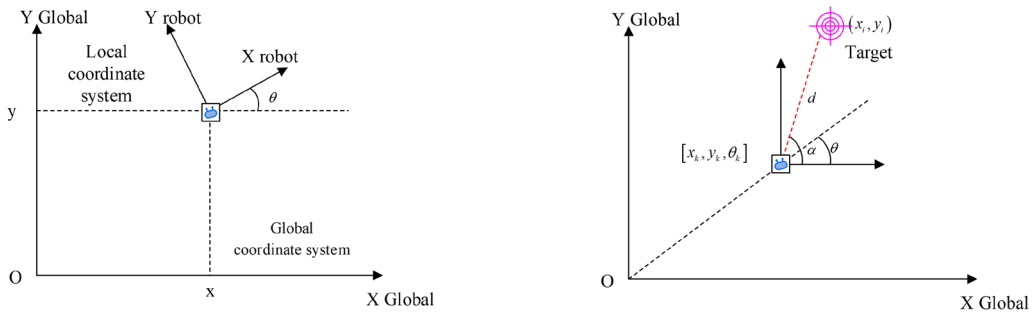

(a) Coordinate system (b) Relative position relationship diagram

Figure 1. Coordinate System and Relative Positional Relationship Diagram of the Robot Kinematic Model

al., 2024). Therefore, the kinematic model of the robot is shown in equation (1):

$$\begin{bmatrix} \dot{x} \\ \dot{y} \\ \dot{\theta} \end{bmatrix} = \begin{bmatrix} \cos\theta & 0 \\ \sin\theta & 0 \\ 0 & 1 \end{bmatrix} \begin{bmatrix} v \\ \omega \end{bmatrix} \tag{1}$$

In equation (1), $\dot{x}$, $\dot{y}$, and $\dot{\theta}$ represent the coordinates and directional quantity after motion, respectively. θ indicates the directional quantity. v and ω represent the linear velocity and centroid angular velocity. In the global coordinate system, the distance between the robot and the target (x_i, y_i) is d. The directional vector of the target is α. The position of the robot at time k is $[x_k, y_k, \theta_k]$. Then, the expression of the robot observation model is shown in equation (2):

$$z_k = \begin{bmatrix} d \\ \alpha \end{bmatrix} = \begin{bmatrix} \sqrt{(x_i - x_k)^2 - (y_i - y_k)^2} \\ \arctan\dfrac{y_i - y_k}{x_i - x_k} - \theta_k \end{bmatrix} \tag{2}$$

The positioning problem of inspection robots, also known as the filtering problem, can be defined as a nonlinear system during the positioning process. The system is often affected by system noise and sensor measurement noise. EKF is an extension of KF, which transforms the nonlinear state estimation problem into a linear problem by linearizing the nonlinear system model and using the framework of KF for recursive estimation. It is suitable for nonlinear systems (Hu & Huang, 2024; Lee, Lee & Yoo, 2024). Therefore, EKF was chosen in this study as the positioning algorithm for robots under multi-sensor conditions. The traditional KF algorithm assumes that the system is a linear system and that the noise follows a Gaussian distribution, which leads to significant limitations for the algorithm. EKF uses Taylor expansion to approximate nonlinear functions, and obtains a linear approximation model by linearizing the state transition function and observation function. The KF algorithm is used for state estimation based on linear model (Li et al., 2023). The positioning algorithm process for the inspection robot is shown in Figure 2.

As shown in Figure 2, the positioning process requires first setting the initial state estimation values and covariance matrices, and predicting the state estimation and covariance matrix (CM) for the next moment based on the system model and control inputs. The prediction formula is shown in equation (3):

$$\begin{cases} \hat{x}_k^- = f(x_{k-1}, u_{k-1}) \\ P_k^- = A_k P_{k-1} A_k^T + Q_k \end{cases} \tag{3}$$

In equation (3), $\hat{x}_k^-$ and $\hat{x}_{k-1}$ represent the prior state estimation value at time k and the posterior state estimation value at time $k-1$, respectively. f represents the state transition function. u_{k-1} represents the control input at time $k-1$. P_k^- and P_{k-1} represent the prior and posterior covariance matrices, respectively. Q_k is the CM of process noise. A_k represents the Jacobian matrix of f. Then, the Kalman gain K_k is calculated, as shown in equation (4):

$$K_k = P_k^- H_k^T \left(H_k P_k^- H_k^T + R_k \right)^{-1} \tag{4}$$

In equation (4), H_k is the Jacobian matrix of the observed function h. R_k is the CM of the observed noise. The observation predictive value $\hat{z}$ and

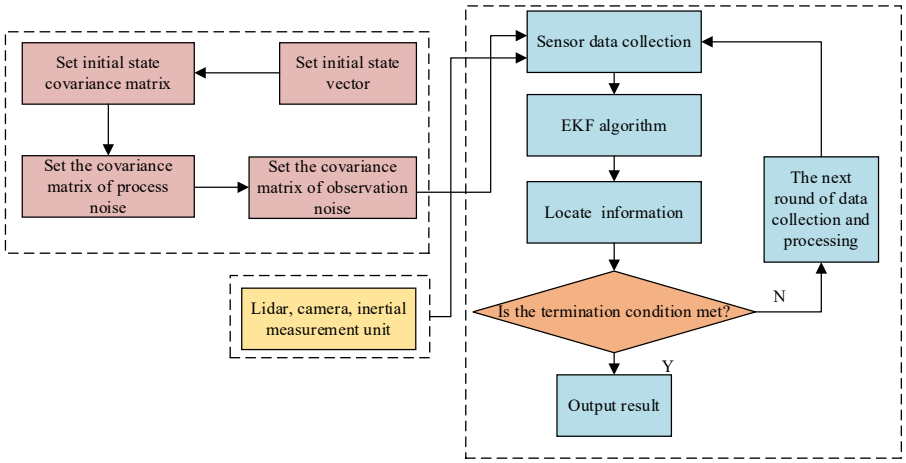

Figure 2. Schematic Diagram of the Positioning Algorithm Flow for the Inspection Robot

residual ε are calculated based on the prior state estimation values, as shown in equation (5):

$$\begin{cases} \hat{z}_k = h\left(\hat{x}_{k/k-1}\right) \\ \varepsilon = z_k - \hat{z}_k \end{cases} \tag{5}$$

In equation (5), Z_k represents the observed value. Finally, the state and covariance are updated based on the KF gain, as shown in equation (6):

$$\begin{cases} \hat{x}_k = x_k^- + K_k\left(z_k - h\left(x_k^-\right)\right) \\ P_k = \left(I - K_k H_k\right) P_k^- \end{cases} \tag{6}$$

The inspection robot regards the pose and environmental feature information as state variables based on the EKF algorithm, and defines the relationship between state variables using error covariance. However, the traditional EKF algorithm achieves the linearization of nonlinear functions through Taylor series expansion, which can easily ignore higher-order terms and lead to a reduced system estimation accuracy or even filter divergence. In response to this, the study introduced the principle of adaptive filtering to optimize the traditional EKF. By employing innovation-based adaptive estimation, the system utilizes the statistical characteristics of the innovation sequence to dynamically estimate and correct the system model in real time, thereby improving the estimation accuracy of the filter. The improved EKF positioning principle is shown in Figure 3.

As shown in Figure 3, the adaptive EKF will calculate the new information based on the difference between the measured and anticipated values. It utilizes the statistical properties of new information to evaluate the performance of filters, achieving the correction of CM Q_k for noise and CM R_k for the observed noise. The adaptive adjustment rule is shown in equation (7):

$$\begin{cases} Q_k^* = K_k A_{k-1} K_k^T \\ e = z_k - z_{k-1} \\ F_k = \dfrac{1}{M}\sum_j^i = e_i e_i^T \\ R_k^* = F_k - H_k \hat{P}_{k/k-1} H_k^T \end{cases} \tag{7}$$

In equation (7), e_i represents the observation innovation, namely the difference between the actual measurement and the predicted observation, serving as an indicator of the prediction error of the filter, while M denotes the matching window (or sliding window size) used for calculating the statistical characteristics of the innovation sequence over the most recent M samples.

3.2 Design of the PP model

The PP of inspection robots relies on accurate positioning information. After providing reliable position information for the inspection robot based on the improved EKF positioning algorithm, a PP model for the robot was designed to support complex inspection tasks. PP is an important component of the autonomous navigation technology for inspection robots, which involves generating an optimal path from the starting point to the endpoint in known or unknown environments based on environmental maps, obstacle distribution, robot dynamics constraints, and task requirements. In this paper, the ACO algorithm was selected for the PP algorithm

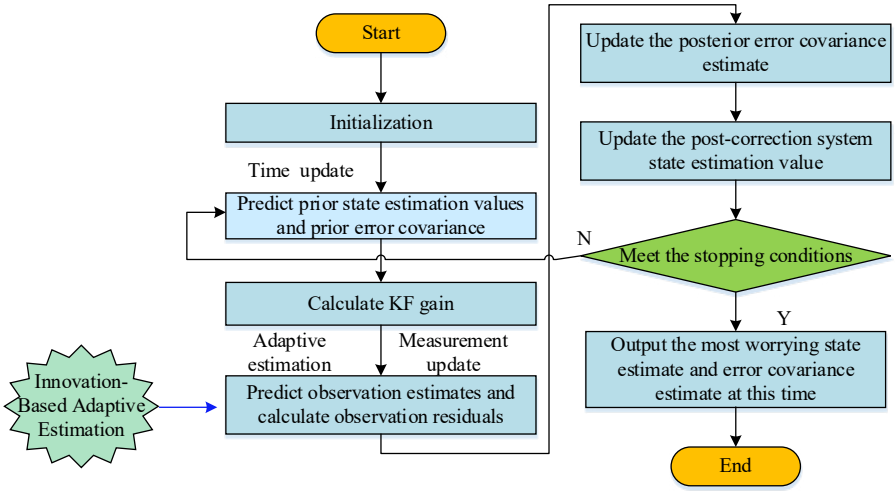

Figure 3. Schematic Diagram of the EKF Algorithm Positioning Principle

design. ACO is a swarm intelligence algorithm that mimics the foraging behavior of ants, simulating their behavior of finding the shortest path by releasing and perceiving pheromones. The working mechanism is shown in Figure 4 (Chen et al., 2024; Li, Yan & Huang, 2024).

As shown in Figure 4, the path with a high concentration of pheromones features a higher probability of leading to the food source. Therefore, over time, the concentration of pheromones on shorter paths will gradually increase, while the concentration of pheromones on longer paths will gradually decrease due to the smaller number of ants on those paths. Hence, ant colonies discover the quickest route from their nest to the food. The build-up of pheromones serves as the ACO algorithm's positive reinforcement mechanism, guiding the search process towards convergence and gradually reaching the best possible solution (Chowdhury et al., 2024; Wang & Feng, 2024). Additionally, in view of this algorithm, multiple ant colonies can perform path search simultaneously, which enables a strong parallelism and distributed characteristics. The PP algorithm first abstractly models the motion environment of the inspection robot and divides the inspection map into different grids. Then, certain parameters are initialized, such as the ant colony count, the pheromone importance, the heuristic function importance factor, the pheromone volatilization factor, etc. During the algorithm iteration process, the ants shall move between different path nodes with a certain probability, which depends on the distance from the current node to adjacent nodes and on the concentration of pheromones on adjacent nodes. The transition probability $p_{ij}^{k}(t)$ calculation is given in equation (8):

$$p_{ij}^{k}(t)=\begin{cases}0\ ,else\\ \dfrac{\left[\tau_{ij}(t)\right]^{\alpha}\bullet\left[\eta_{ij}(t)\right]^{\beta}}{\sum_{j\in allowed_k}\left[\tau_{ij}(t)\right]^{\alpha}\bullet\left[\eta_{ij}(t)\right]^{\beta}} & j\in allowed_k\end{cases} \quad (8)$$

In equation (8), $\tau_{ij}(t)$ represents the pheromone concentration between the nodes i and j. t is the moment when the ant colony leaves $\tau_{ij}(t)$, and the initial pheromone concentration is $\tau_{ij}(0)=C$. α represents the heuristic factor of pheromone concentration, and the value of α determines the importance of pheromone concentration in path selection. β represents the expected heuristic factor, which determines whether the path selection should be based on pheromones. $\eta_{ij}(t)$ represents the path heuristic value. Over time, the ACO algorithm will simulate the phenomenon of natural dissipation of pheromones in nature, and introduce the volatility coefficient ρ to help the algorithm avoid premature convergence. A smaller volatility coefficient ρ corresponds to a slower volatilization of pheromones, and ACO tends to utilize the known information. A higher volatility coefficient ρ increases the possibility of ACO exploring unknown paths. The process of pheromone change is shown in equation (9):

$$\begin{cases}\tau_{ij}(t+n)=(1-\rho)*\tau_{ij}(t)+\triangle\tau_{ij}(t)\\ \triangle\tau_{ij}(t)=\sum_{k=1}^{m}\triangle\tau_{ij}^{k}(t)\end{cases} \quad (9)$$

In equation (9), m is the total number of ant colonies, $k=\{1,2,3,...,m\}$. The calculation of the pheromone increment $\triangle\tau_{ij}(t)$ is given in equation (10):

$$\triangle\tau_{ij}(t)\begin{cases}\dfrac{Q}{L_k} & tour(i,j)\in tour_k\\ 0\ else\end{cases} \quad (10)$$

In equation (10), Q represents the strength of pheromones, while L_k represents the total length of the paths explored by ants during the iteration process. The initial pheromone concentration in the context of the conventional ACO algorithm is uniformly distributed, which increases the randomness of path selection and makes it difficult for the algorithm to effectively explore the solution space in the initial stage. Meanwhile, the residual pheromones also make it difficult for the algorithm to escape from local optima (Banciu et al., 2024). In this regard, research was conducted to improve

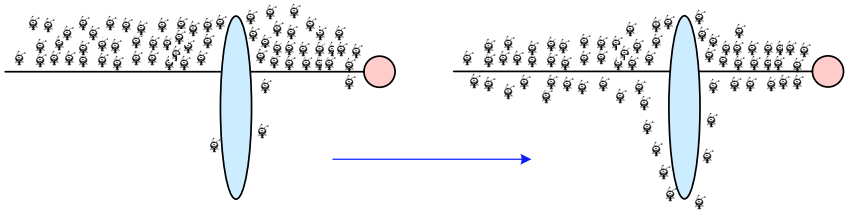

Figure 4. Illustrative Layout of the Working Principle of the Ant Colony Algorithm

the ACO algorithm, and a PP model for inspection robots was constructed as shown in Figure 5.

As shown in Figure 5, the Bidirectional Particle Swarm Optimization (BPSO) algorithm is employed to optimize the distribution of initial pheromones. BPSO introduces a bidirectional learning mechanism based on Particle Swarm Optimization (PSO) algorithm, where one particle in PSO represents a candidate solution, and its position and velocity are iteratively updated to approximate the optimal solution. BPSO considers both the actual and inverse estimates of particles, that is, simultaneously recording the optimal value p_d and the worst value pp_d of particles, and introducing the inverse particle $\widetilde{p_d}$ of p_d as a new learning factor for BPSO during the iteration process. The learning process is shown in equation (11):

$$v_{id}(t+1) = \omega v_{id}(t) + c_1 rand(p_{id}(t) - x_{id}(t)) + c_2 rand(p_{gd}(t) - x_{id}(t)) + c_3 rand(\widetilde{pp_{gd}} - x_{id}(t)) \quad (11)$$

In equation (11), v_{id} and x_{id} are particle velocity and position, respectively. c_1, c_2 and c_3 represent the learning factors. p_{gd} is the global optimal value, while pp_{gd} represents the global worst value. p_{id} represents the individual optimal value and ω is the weight.

In addition, the traditional ACO algorithms feature a strong dependence on pheromones and a high sensitivity to algorithm parameters. This study introduces an adaptive mechanism to enable the algorithm to dynamically adjust its parameters and strategies based on the current search state, thereby improving the robustness and adaptability of the algorithm. The study related the parameters α and β specific to individual ants in the ant colony to their respective adjustment parameters c_1, c_2 and c_3, which regulated the behavioral characteristics of ant individuals. The transition probability calculation process is expressed in equation (12):

$$p_{ij}^k(t) = \begin{cases} 0, else \\ \dfrac{[\tau_{ij}(t)]^{\alpha(c)} \cdot [\eta_{ij}(t)]^{\beta(c)}}{\sum_{j \in allowed_k} [\tau_{ij}(t)]^{\alpha(c)} \cdot [\eta_{ij}(t)]^{\beta(c)}} & j \in allowed_k \end{cases} \quad (12)$$

Finally, the study introduces the quadratic path smoothing algorithm, which adjusts the position of path points based on the principle of quadratic programming to achieve a higher smoothness of the path under certain constraints. The operation mechanism is shown in Figure 6.

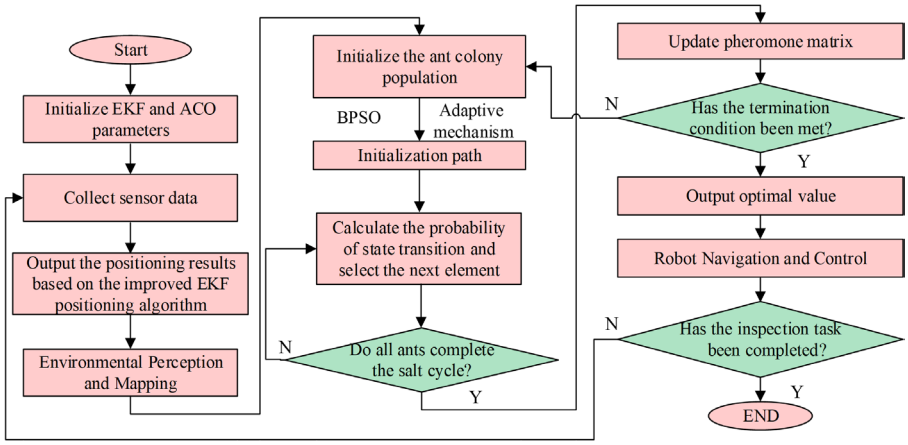

Figure 5. PP Model for Inspection Robots Based on an Improved ACO algorithm

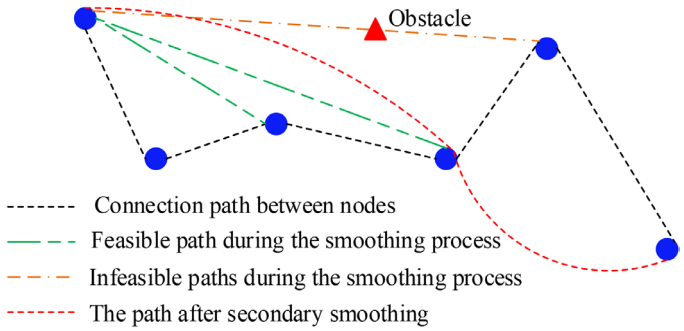

Figure 6. Illustrative Layout of the Working Mechanism of the quadratic path smoothing algorithm

4. Experiments and Results

To assess the efficacy of the inspection control technology for inspection robots proposed in this paper, performance testing for positioning algorithms and application analysis experiments for PP models were conducted, and the results were analyzed and discussed.

4.1 Experiment for the MSF Positioning Algorithm

The experiment was conducted on a Windows 10 operating system, using Python 3.8.8 as the programming language and Python 1.8.1 as the deep learning framework. The central processing unit was Intel (R) Core (TM) i5-7200 CPU@2.50GHz. The memory was 64.00GB, and the image processor was Ge Force RTX 2080Ti. Performance testing was conducted on the positioning algorithm using the KITTI dataset, MH dataset, and TUM dataset, which include different scenarios and sensor configurations, to evaluate the performance of the positioning algorithm in static and dynamic scenarios. The test compared the multi-method integration model in (Jiang et al., 2023), the closed-loop KF algorithm in (Li, 2024), and the RFID tag array positioning method in (Xie et al., 2024). The root mean square error (RMSE) and mean absolute error (MAE) results for four positioning algorithms are shown in Figure 7. As shown in Figure 7(a), for different anchor points, the improved EKF algorithm proposed in this paper obtained the lowest RMSE value, which is a significant advantage with regard to the positioning accuracy in comparison with the other three models. The minimum RMSE value for the improved EKF algorithm was 0.136, while the RMSE values for the other methods were all higher than 0.25. Further on, as shown in Figure 7(b), the MAE values for the other three employed models at different anchor points showed consistent patterns, and the MAE value for the improved EKF algorithm was the smallest. Based on these two error indicators, the improved EKF algorithm achieved the highest positioning accuracy for the inspection robot.

Further on, the relative rotation error (RRE) and absolute trajectory error (ATE) results for the four positioning models are shown in Figure 8. As shown in Figures 8(a) and 8(b), in comparison with the other three advanced positioning algorithms, the improved EFK method proposed

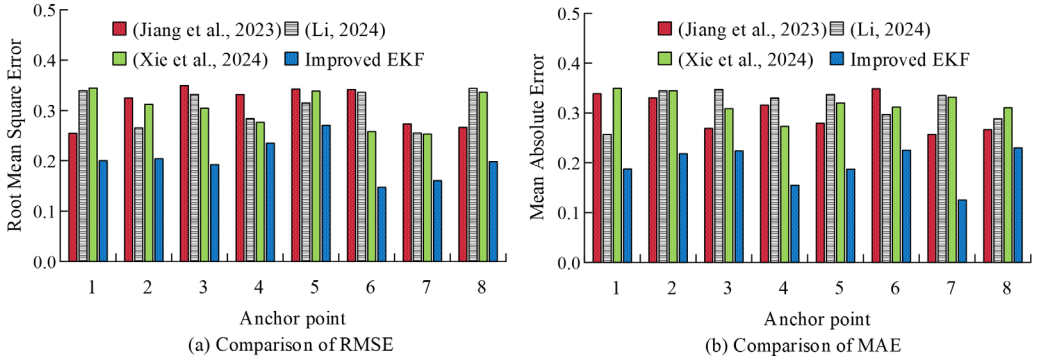

Figure 7. Comparison of the Positioning Accuracy for the Four Models

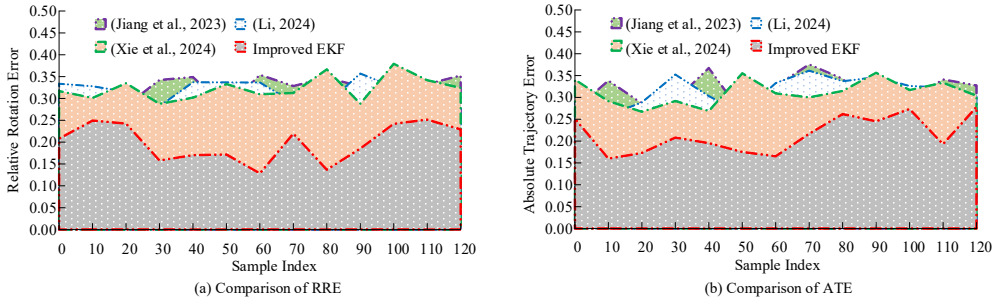

Figure 8. Comparison of RRE and ATE for the Four Location Models

in this study significantly reduced the ATE and RRE values, with a minimum ATE value of 0.160 and a minimum RRE value of 0.137. The ATE and RRE values for the other three methods fluctuated above the 0.25 value level, indicating that the proposed algorithm achieved a high positioning accuracy for the inspection robot in the global coordinate system, which confirmed the stability and accuracy of the improved EFK method under long-term and long-distance operation.

The success rate and timeliness rate for the four employed positioning algorithms are represented in Figure 9. In Figure 9(a), the localization success rate for the improved EKF algorithm increased with the number of iterations and converged to a maximum value of 0.957. The success rates of location detection for the other three positioning algorithms were all below 0.85. As represented in Figure 9(b), the improved EKF algorithm obtained the best timeliness rate and featured significant advantages in comparison with the other methods, as it could complete localization in a shorter time.

4.2 Experiment for the PP Model

In this study, the pheromone volatilization coefficient ρ was set at 0.3 and the heuristic factor of the ant colony algorithm β = α = 1, with a population size of 60 and a maximum number of 200 iterations, to complete PP performance testing in a 30*30 grid environment. Firstly, the performance of the improved ACO algorithm proposed in this paper was tested using the Schwefel, Rosenbrock, Griewank, and Ackley functions as test functions to evaluate the hypervolume (HV) and the uniformity of performance (UP) for three algorithms, namely the improved ACO algorithm, the traditional ACO algorithm and the genetic algorithm (GA). The experiment outcomes are represented in Figure 10. As shown in Figure 10(a), the improved ACO algorithm quickly reached and maintained a HV value close to 1.0. By introducing the BPSO algorithm for optimizing the initial pheromone distribution, the algorithm's global search ability was enhanced and the diversity of the solution

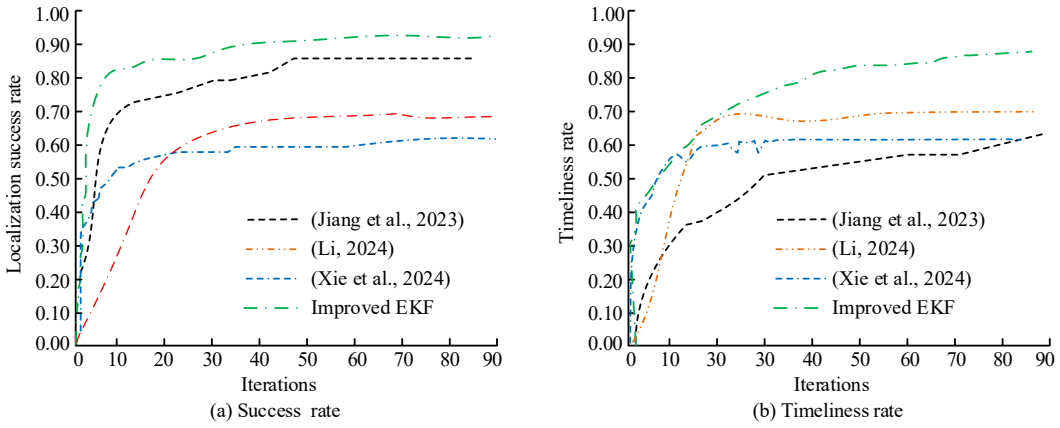

Figure 9. Comparison of the Success Rate and Immediacy for the Four Positioning Algorithms

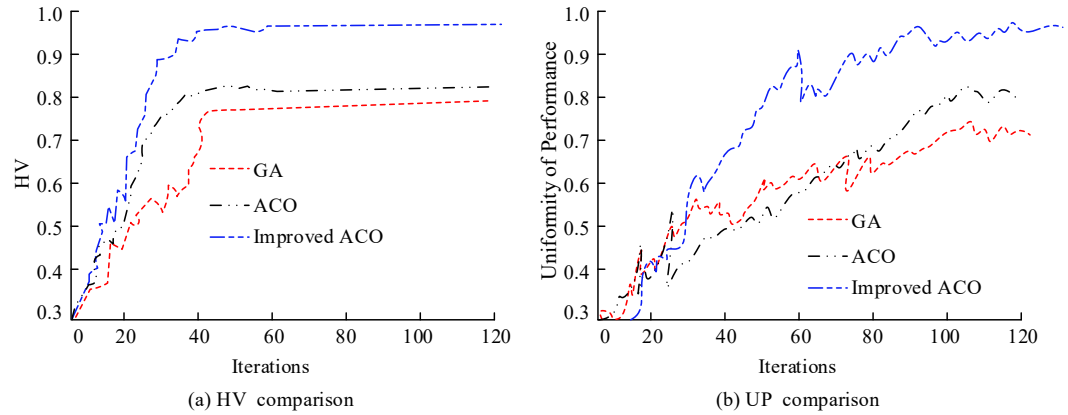

Figure 10. Comparison of the HV and UP Values for the Three Employed Algorithms

set was improved. The search and optimization capabilities of the other two algorithms were insufficient, resulting in a significant decrease in HV values. As shown in Figure 10(b), the UP value for the improved ACO algorithm increased rapidly with the number of iterations and converged to a maximum value of 0.943. The UP values for the traditional ACO algorithm and GA remained stable at around 0.7 and 0.6, respectively. The adaptive improvement strategy enhanced the robustness and adaptability of the ACO algorithm, thereby improving the uniformity of the obtained solution.

Further on, the improved ACO PP model proposed in this paper was compared with the improved RRT* algorithm based on Tang et al. (2024)., the improved A* algorithm based on Xi et al. (2024), and the NNE-DRL adaptive PP model based on Lou et al. (2025). The experiment involved a railway inspection environment with obstacles for testing the planning performance. The planning and efficiency comparison results for the four above-mentioned models are shown in Figure 11. As shown in Figure 11(a), the path length planned by the improved ACO algorithm was the shortest, and the path length obtained after 70 iterations was 10.299 m. The shortest path lengths planned by the improved RRT*, improved A*, and NNE-DRL models were 15.311 m, 15.445 m, and 16.397 m, respectively. The maximum decrease in the shortest path length reached 36.49%. The adaptive mechanism and BPSO enhanced the search capability of the improved ACO algorithm, enabling it to find better paths. As shown in Figure 11(b), the improved ACO algorithm obtained the shortest planning time, taking only 51.975 seconds to complete PP. In comparison with the other three methods, the planning time was reduced by up to 46.67 seconds, and the optimal path was found in a shorter time. Therefore, the improved ACO algorithm proposed in this paper achieved a higher comprehensive planning performance.

Finally, the smoothness and success rate related to PP for inspection robots in actual operations were compared, as shown in Figure 12. As shown in Figure 12(a), in the presence of obstacles, the path planned by the improved ACO algorithm was the smoothest, with smoothness fluctuating within the range of 0.80-0.95, which was significantly better than for the other three methods. As shown in Figure 12(b), the maximum success rate of PP for the improved ACO algorithm was 0.973. The adaptive strategy and BPSO proposed in this paper contribute to enhancing the ACO algorithm's optimization capability in solving the path planning problem for inspection robots, particularly by improving the global search ability, convergence speed, and solution stability in complex obstacle environments.

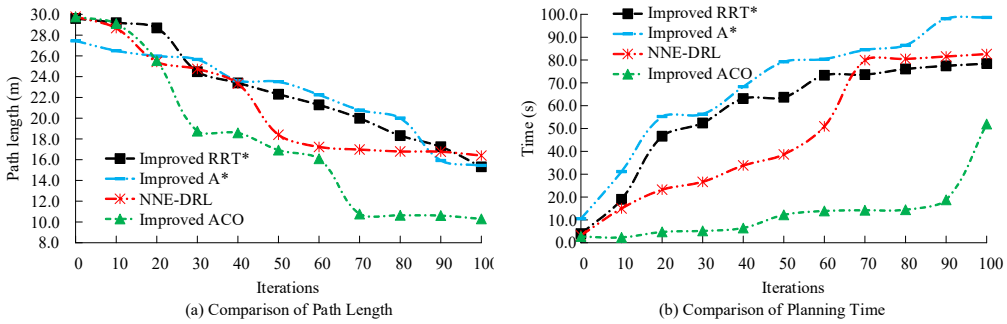

Figure 11. Comparison of Path Length and Planning Time for the Four Employed Models

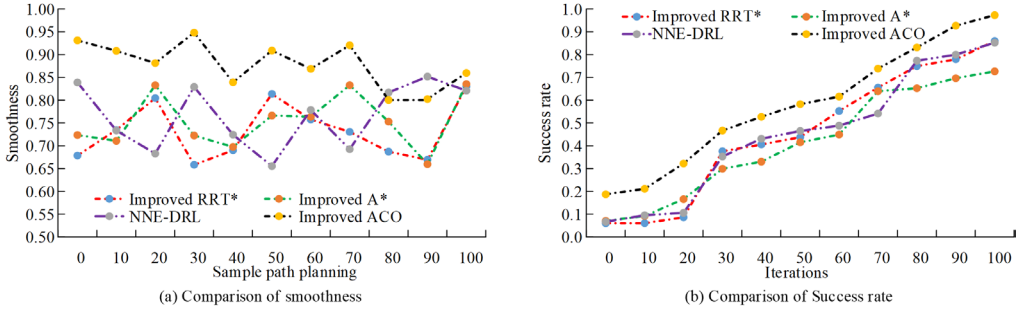

Figure 12. Comparison of the Planning Quality for the Four Employed PP Algorithms

5. Conclusion

To enhance the security and effectiveness of robot inspection and provide solid support for railway transportation, this paper proposed positioning and PP algorithms for railway inspection robots based on improved EKF and ACO, respectively. The experimental outcomes indicated that the improved EKF algorithm reached a high positioning accuracy, achieving a RMSE value of 0.136 and a MAE value of 0.143. In comparison with other employed algorithms, the values of ATE and RRE obtained by the proposed algorithm provided significant advantages and enabled a higher positioning accuracy in the global coordinate system. Additionally, this positioning method obtained a high positioning success rate and immediacy, with a positioning success rate of up to 0.957 and an immediacy index higher than 0.9, which enabled it to achieve an accurate positioning in a short period of time. The improved ant colony optimization algorithm demonstrated a superior optimization capability across multiple benchmark test functions, particularly in solving complex path planning problems for railway inspection robots and the maximum reduction of the length of the planned inspection path reached 36.49%. This model needed only 51.975 seconds to complete the PP In addition, this PP algorithm achieved a high success rate and a high smoothness of robot paths. The model proposed in this paper can help railway inspection robots complete inspection tasks more quickly and improve the inspection efficiency.

Although the proposed MSF positioning algorithm and the improved ACO PP model demonstrated a high performance in various simulation scenarios, their applicability in real-world railway inspection environments still requires further verification. The current experiments were conducted under idealized conditions and did not fully consider practical environmental factors such as complex railway terrains, variable lighting, extreme weather, and obstacle interference, all of which could significantly affect sensor stability, localization accuracy, and path continuity. Additionally, while the improved ACO algorithm proved advantageous with regard to the convergence speed and global search ability for small- to medium-scale tasks, its performance for large-scale, high-density PP tasks remains insufficiently evaluated, particularly regarding the computational complexity and convergence time. Moreover, the current research mainly focuses on algorithm design and simulation validation, without completing the hardware–software integration or collaborative testing on embedded platforms, which may result in challenges related to real-time performance, resource constraints, and power consumption.

From an ethical perspective, although the proposed system does not involve direct interaction with human operators or personal data collection, future deployment scenarios may include operation in human-populated areas or environments requiring spatial coordination or interaction with human workers. In such cases, operational safety, privacy protection, behavior explainability, and regulatory compliance must be carefully addressed. To overcome these limitations, future work will focus on five main directions: (1) conducting field experiments in actual railway environments to evaluate the robustness of localization and PP of railway inspection robots under complex conditions; (2) implementing algorithm migration and system integration on embedded hardware platforms to improve a system`s real-time performance and deployment adaptability; (3) further optimizing ACO parameter adjustment mechanisms and path smoothing strategies to enhance generalization and solution stability in complex tasks; (4) developing extended models for multi-robot task allocation and collaborative PP for improving system scalability; and (5) incorporating ethical assessment frameworks and human–robot collaboration safety mechanisms to ensure a secure and compliant large-scale deployment, that is, the real-world integration and implementation of the proposed algorithms in practical railway inspection robot systems. These improvements will lay a solid foundation for the deployment and intelligent advancement of railway inspection robots.

Acknowledgements

The acknowledgements corrected to:This research was supported by the Henan Provincial Vocational Education Teaching Reform Research and Practice Project "Research and Practice on Cultivating Students' Technological Innovation Ability Based on Embedded Application Technology" (Project No.: ZJA20115); the Henan Provincial Key Science and Technology Project "Key Technology Research and Development of Intelligent Inspection Robot for Rail Transit Based on Digital Twin" (Project No.: 252102221015); and the Henan Provincial Key Scientific and Technological Project "Research and Development of Key Technologies for AI-Based SLAM Intelligent Robots" (Project No.: 212102210281).

REFERENCES

Banciu, D., Petrescu, A.-G., Oncioiu, I. et al. (2024) The Simulation Framework for Automated Trading Algorithms on Capital Markets. *Studies In Informatics and Control*. 33(4). https://doi.org/10.24846/v33i4y202405.

Chen, S., Li, G., Chang, K., et al. (2024) Ultra-short-term Load Forecasting Based on XGBoost-BiGRU. International Journal of Computers, Communications & Control. 19(5), Art. ID 6631. https://doi.org/10.15837/ijccc.2024.5.6631.

Chowdhury, A. R., Hazra, J., Dasgupta, K. et al. (2024) Fuzzy rule-based hyperspectral band selection algorithm with ant colony optimization. *Innovations in Systems and Software Engineering*. 20(2), 161-174. https://doi.org/10.1007/s11334-021-00432-4.

Cid, A., Vangasse, A., Campos, S. et al. (2024) Wireless Communication-aware Path Planning and Multiple Robot Navigation Strategies for Assisted Inspections. *Journal of Intelligent & Robotic Systems*. 110(2), Art. ID 88. https://doi.org/10.1007/s10846-024-02112-4.

Fan, J. K. (2024) A Simulation Study on Inland Container and Truck Scheduling Optimization. *International Journal of Simulation Modelling*. 23(4), 680-691. https://doi.org/10.2507/IJSIMM23-4-CO16.

Gilmour, A., Jackson, W., Zhang, D. et al. (2023) Robotic Positioning for Quality Assurance of Feature-Sparse Components Using a Depth-Sensing Camera. *IEEE Sensors Journal*. 23(9), 10032-10040. https://doi.org/10.1109/JSEN.2023.3258899.

Hu, R. & Huang, P. (2024) Autonomous Driving Decision-Making Based on an Improved Actor-Critic Algorithm. *Studies in Informatics and Control*. 33(4), 37-50. https://doi.org/10.24846/v33i4y202404.

Jiang, Y., Yu, Y., Sun, R. et al. (2023) Research on dynamic path planning method of electric inspection robot based on fuzzy neural network. *Energy Reports*. 9(8), 483-491. https://doi.org/10.1016/j.egyr.2023.04.308.

Jovanović, V., Marinković, D., Janoević, D. et al. (2023) Influential Factors in the Loading of the Axial Bearing of the Slewing Platform Drive in Hydraulic Excavators. *Tehnički Vjesnik* [*Technical Gazette*]. 30(1), 158-168. https://doi.org/10.17559/TV-20220425205603.

Lee, J.-H., Lee, J.-K. & Yoo, S.-G. (2024) An Empirical Study of Success Factors in Korea's Game Industry. *Computer Science and Information Systems*. 21(2), 525-545. https://doi.org/10.2298/CSIS221117009L.

Li, S., Zheng, C., Shi, Y. et al. (2023) A Test Case Generation Method for Workflow Systems Based on I/O WF_Net. *Tehnički Vjesnik* [*Technical Gazette*]. 30(1), 235-240. https://doi.org/10.17559/TV-20220822145848.

Li, Y. (2024) Constructing the intelligent expressway traffic monitoring system using the internet of things and inspection robot. *Journal of Supercomputing*. 80(7), 8742-8766. https://doi.org/10.1007/s11227-023-05794-z.

Li, L., Jiang, L., Tu, W. et al. (2024) Smooth and Efficient Path Planning for Car-Like Mobile Robot Using Improved Ant Colony Optimization in Narrow and Large-Size Scenes. *Fractal and Fractional*. 8(3), Art. ID 157. https://doi.org/10.3390/fractalfract8030157.

Li, W., Yan, X. & Huang, Y. (2024) Cooperative-Guided Ant Colony Optimization with Knowledge Learning for Job Shop Scheduling Problem. *Tsinghua Science and Technology*. 29(5), 1283-1299. https://doi.org/10.26599/TST.2023.9010098.

Lou, T., Yue, Z., Chen, Z. et al. (2025) A hybrid multi-strategy SCSO algorithm for robot path planning. *Evolving Systems*. 16, Art. ID 54. https://doi.org/10.1007/s12530-025-09680-2.

Moon, J., Son, M., Oh, B. et al. (2024) Automatic Voltage Stabilization System for Substation using Deep Learning. *Computer Science and Information Systems*. 21(2), 437-452. https://doi.org/10.2298/CSIS220509050M.

Pang, Z., Wang, Y. & Yang, F. (2024) Application of Optimized Kalman Filtering in Target Tracking Based on Improved Gray Wolf Algorithm. *Scientific Reports*. 14(1), Art. ID 8955. https://doi.org/10.1038/s41598-024-59610-6.

Stanojević, B. & Stanojević, M. (2024) On approaching full fuzzy data envelopment analysis and its validation. *International Journal of Computers, Communications & Control*. 19(6), Art. ID 6855. https://doi.org/10.15837/ijccc.2024.6.6855.

Sugin Elankavi, R., Dinakaran, D., Doss, A. S. A., et al. (2023) Design of a wheeled-type In-Pipe Inspection Robot to overcome motion singularity in curved pipes. *Journal of Ambient Intelligence and Smart Environments*. 16(1), 43-55. https://doi.org/10.3233/AIS-220247.

Tang, J., Pan, Q., Chen, Z. et al. (2024) An Improved Artificial Electric Field Algorithm for Robot Path Planning. *IEEE Transactions on Aerospace and Electronic Systems*. 60(2), 2292-2304. https://doi.org/10.1109/TAES.2024.3351110.

Wang, W., Qu, R., Liao, H. et al. (2023) 5G MEC-based Intelligent Computation Offloading in Power Robotic Inspection. *IEEE Wireless Communications*. 30(2), 66-74. https://doi.org/10.1109/MWC.003.2200350.

Wang, W. & Feng, L. (2024) Robust image watermarking using ant colony optimization and fast generic radial harmonic Fourier moment calculation. *IET Image Processing*. 18(5), 1200-1212. https://doi.org/10.1049/ipr2.13019.

Xi, M., Dai, H., He, J. et al. (2024) A Lightweight Reinforcement-Learning-Based Real-Time Path-Planning Method for Unmanned Aerial Vehicles. *IEEE Internet of Things Journal*. 11(12), 21061-21071. https://doi.org/10.1109/JIOT.2024.3350525.

Xie, Y., Wang, X., Lin, P. et al. (2024) Relative Positioning of the Inspection Robot Based on RFID Tag Array in Complex GNSS-Denied Environments. *IEEE Transactions on Instrumentation and Measurement*. 73, Art. ID 5503214. https://doi.org/10.1109/TIM.2024.3412203.

Xing, H. R. (2024) Optimizing Human-Machine Systems in Automated Environments. *International Journal of Simulation Modelling*. 23(4), 716-727. https://doi.org/10.2507/IJSIMM23-4-CO19.